Numerically Simulating Non-Gaussian Sea Surfaces

By Barry Vanhoff,[1] Steve Elgar,[2] and R. T. Guza[3]

Abstract: A technique to simulate non-Gaussian time series with a desired ("target") power spectrum and bispectrum is applied to ocean waves. The targets were obtained from observed bottom pressure fluctuations of shoaling, nonbreaking waves in 2–9 m water depth. The variance (i.e., frequency integrated spectrum), skewness, and asymmetry (i.e., frequency integrated bispectrum) of the simulated time series compare favorably with the observations, even for highly skewed and asymmetric near-breaking waves. The mean lengths of groups of high waves from non-Gaussian simulated time series are closer to observed values than those from Gaussian simulations. The simulations suggest that quadratic phase coupling between waves (of different frequencies) in shallow water results in longer wave groups than occur with linear, uncoupled waves having the identical power spectrum.

INTRODUCTION

In this study, a method for generating numerical realizations of quadratically nonlinear (e.g., non-Gaussian) time series with a specified ("target") power spectrum and bispectrum (Vanhoff and Elgar 1997) is applied to ocean surface waves. Low amplitude waves have linear dynamics and Gaussian statistics. Realizations of Gaussian sea-surface elevation time series with a specified power spectrum can be generated numerically by coupling Fourier amplitudes (determined by the spectrum) with independent, random phases (Rice 1954; Andrew and Borgman 1981). However, in intermediate-depth and shallow water ($kh \le 1$, where k is a representative wave number and h is the depth) quadratic interactions between even moderately energetic Fourier components of the wave field result in non-Gaussian statistics that are described by the bispectrum (Hasselmann et al. 1963). The non-Gaussian properties of the sea surface are not reproduced by a linear combination of Fourier components with random phases, but can be approximated by numerical simulations that reproduce both the observed amplitudes (e.g., power spectrum) and the quadratic phase coupling between components (e.g., bispectrum).

Techniques to generate realizations of linear (Gaussian) and quadratically phase coupled (non-Gaussian) random processes are briefly reviewed in the next section. Target power spectra and bispectra are based on observations of nonbreaking ocean waves in 2–9 m water depth. Next it is shown that the variance, skewness, and asymmetry of numerically simulated sea-surface elevation time series compare favorably to the observed statistics even for nearly breaking waves. It is shown in the following section that observed mean lengths of groups of high waves (mean run length) in shallow water are predicted better by non-Gaussian than by Gaussian simulations, and that quadratic nonlinear interactions increase the mean run length. Conclusions follow.

NUMERICAL SIMULATION OF SEA-SURFACE ELEVATION TIME SERIES

A discretely sampled sea-surface elevation time series $x(n)$ can be represented as (Rice 1954)

$$x(n) = \sum_{k=1}^{K} C_k \cos(2\pi f_k n + \phi_k) \tag{1}$$

where $2K$ = number of samples; $f_k = kf_N/K$; and f_N = Nyquist frequency. The Fourier amplitude C_k at frequency f_k is

$$C_k = [2P(f_k)]^{1/2} \tag{2}$$

where $P(f_k)$ = the power spectrum of $x(n)$, defined by

$$P(f_k) = E[|X(f_k)|^2] \tag{3}$$

where the $X(f_k)$ = discrete Fourier coefficients of $x(n)$; and $E[\,]$ = expected value, or average, operator. If the Fourier phases ϕ_k are random and uniformly distributed on $[0, 2\pi)$ and $K >> 1$, then $x(n)$ has Gaussian statistics (Rice 1954). Realizations of a Gaussian sea surface with a specified power spectrum $P(f_k)$ can be generated by coupling the amplitudes C_k with random phases ϕ_k [(1)].

An alternative representation to (1) is

$$x(n) = \sum_{k=1}^{K} a_k \cos(2\pi f_k n) + b_k \sin(2\pi f_k n) \tag{4}$$

where a_k, b_k = independent Gaussian distributed random variables with zero mean and variance $P(f_k)$. As $K \rightarrow \infty$ statistics of sea surfaces generated with (1) are identical to those using (4) (Rice 1954). For power spectral shapes typically observed in the ocean, (1) and (4) produce sea surfaces with similar statistics for K as low as 32 (Elgar et al. 1985).

Nonrandom phase relationships between triads of Fourier components (with frequencies f_l, f_m, f_{l+m}) of a non-Gaussian random process characterized by quadratic nonlinearities are described statistically by the bispectrum $B(f_l, f_m)$ (Hasselmann et al. 1963). For a discretely sampled process (Haubrich 1965; Kim and Powers 1979)

$$B(f_l, f_m) = E[X(f_l)X(f_m)X^*(f_l + f_m)] \tag{5}$$

If the three Fourier components on the right-hand side of (5) are independent of each other (e.g., their phases are random as in a Gaussian process), $B(f_l, f_m) = 0$. Owing to symmetry relations, $B(f_l, f_m)$ is completely defined by its values in a triangle in (f_l, f_m)-space with vertices at (0, 0), $(f_{N/2}, f_{N/2})$, and $(f_N, 0)$ (Hasselmann et al. 1963). See Nikias and Raghuveer (1987) and Elgar and Chandran (1993) for reviews of bispectra.

Time series with nonzero bispectra cannot be simulated accurately using (1) or (4). However, a quadratically phase-coupled time series [with Fourier coefficients $\hat{X}(f_k)$, and specified power spectrum and bispectrum] can be generated by passing a Gaussian process [produced by (1) or (4)] through the quadratic filter (Vanhoff and Elgar 1997)

[1] Res. Assoc., School of Electrical Engrg. and Comp. Sci., Washington State Univ., Pullman, WA 99164-2752.

[2] Prof., School of Electrical Engrg. and Comp. Sci., Washington State Univ., Pullman, WA.

[3] Prof., Ctr. for Coast. Studies, Univ. of California, 9500 Gilman Dr., La Jolla, CA 92093-0209.

Note. Discussion open until September 1, 1997. To extend the closing date one month, a written request must be filed with the ASCE Manager of Journals. The manuscript for this paper was submitted for review and possible publication on April 1, 1996. This paper is part of the ***Journal of Waterway, Port, Coastal, and Ocean Engineering***, Vol. 123, No. 2, March/April, 1997. ©ASCE, ISSN 0733-950X/97/0002-0068–0072/$4.00 + $.50 per page. Paper No. 12891.

$$\hat{X}(f_k) = G(f_k) + \sum_{f_l=-f_N}^{f_N} Q(f_l, f_k - f_l)G(f_l)G(f_k - f_l); \quad -f_N \le f_k \le f_N \tag{6}$$

where $G(f_k) = G^*(-f_k)$ are Fourier coefficients of a Gaussian realization with target power spectrum $P(f_k)$; and $Q(f_l, f_m)$ = the second-order Volterra kernel (Schetzen 1980), given in terms of $B(f_l, f_m)$ in (9).

The power spectrum [(3)] of a time series simulated using (6) is

$$\hat{P}(f_k) = E[|G(f_k)|^2] + \sum_{f_l=-f_N}^{f_N} |Q(f_l, f_k - f_l)|^2 E[|G(f_l)|^2]E[|G(f_k - f_l)|^2]$$

$$= P(f_k) + \sum_{f_l=-f_N}^{f_N} |Q(f_l, f_k - f_l)|^2 P(f_l)P(f_k - f_l); \quad -f_N \le f_k \le f_N \tag{7}$$

Cross-product terms proportional to $E[G(f_k)G^*(f_l)G^*(f_k - f_l)]$ and its conjugate do not appear in (7) because these are identically zero for the Gaussian $G(f_k)$. By constraining Q to have the same symmetry properties as the bispectrum, the simulated bispectrum [using (6) in (5)] becomes (Vanhoff and Elgar 1997)

$$\hat{B}(f_l, f_m) = 2Q^*(f_l, f_m)[P(f_l)P(f_m) + P(f_l)P(f_l + f_m)$$

$$+ P(f_m)P(f_l + f_m)] + 8 \sum_{f_a=-f_N}^{f_N} Q(f_a, f_l - f_a)Q(-f_a, f_m + f_a)$$

$$\times Q^*(f_l - f_a, f_m + f_a)P(f_a)P(f_l - f_a)P(f_m + f_a);$$

$$-f_N \le f_l, f_m \le f_N \tag{8}$$

Equating the target bispectrum B [(5)], to the simulated bispectrum $\hat{B}$ [(8)], assuming the last term in (8) is small (discussed in the following), and solving for Q yields

$$Q(f_l, f_m) = \frac{B^*(f_l, f_m)}{2[P(f_l)P(f_m) + P(f_l)P(f_l + f_m) + P(f_m)P(f_l + f_m)]} \tag{9}$$

Summarizing, to generate a realization of a random process with power spectrum P and bispectrum B, a Gaussian time series with power spectrum P [generated using (1) or (4)] is passed through a quadratic filter [(6)] specified by P and B [(9)]. By repeating the process with new sets of random phases, independent realizations of a non-Gaussian time series are produced.

The simulated power spectrum and bispectrum are not generally identical to their respective targets. For a time series with nonzero bispectrum, the terms within the summation in (7) are positive definite, and thus simulated power spectral levels $\hat{P}(f_k)$ [(7)] exceed the target values $P(f_k)$. These errors can be eliminated by modifying (7), but the fidelity of the simulated bispectrum is degraded.

For a process with a single phase-coupled triad ($f_l, f_m, f_l + f_m$), the error in $\hat{P}(f_l + f_m)$ depends on $|Q(f_l, f_m)|^2$ and the magnitude of $P(f_l)$ and $P(f_m)$. In the worst case of relatively low $P(f_l + f_m)$

$$\hat{P}(f_l + f_m) \approx P(f_l + f_m)[1 + b^2(f_l, f_m)] \tag{10}$$

where $b(f_l, f_m)$ = bicoherence (Haubrich 1965, Kim and Powers 1979)

$$b(f_l, f_m) = \frac{|B(f_l, f_m)|}{\sqrt{P(f_l)P(f_m)P(f_l + f_m)}} \tag{11}$$

The bicoherence indicates the relative amount of quadratic phase coupling among the components of a triad. For no phase coupling, $b(f_l, f_m) = 0$ and $\hat{P}(f_l + f_m) = P(f_l + f_m)$. On the other hand, if all the energy at $f_l + f_m$ is phase coupled to that at f_l and f_m, then $b(f_l, f_m) = 1$ and $\hat{P}(f_l + f_m) \approx 2P(f_l + f_m)$. In general, the error in the simulated power spectrum is a sum of errors from many partially phase-coupled triads (Vanhoff and Elgar 1997).

The error in the simulated bispectrum $\hat{B}(f_l, f_m)$, equal to the summation term on the right-hand side of (8), has contributions proportional to the sum of products of bicoherences of triads containing at least one of f_l, f_m, or $f_l + f_m$ (Vanhoff and Elgar 1997). For the case of a single phase-coupled triad, the error in $\hat{B}$ is identically zero. With many partially phase-coupled triads the error in the simulated bispectrum can be large or small, depending on whether contributions from different terms cancel. For the ocean wave data considered below, the errors in $\hat{P}$ and $\hat{B}$ are not large.

VERIFICATION OF SIMULATION METHODOLOGY

To test the applicability of the methodology to nonlinear ocean waves, statistics of simulated sea surfaces were compared with those from observations made in shallow water (depths between 2 and 9 m) near Santa Barbara, Calif., and near Duck, N.C. Spectra and bispectra of the observed time series were estimated from 8,192 s records of bottom pressure (sampled at 2 Hz) converted to sea-surface elevation using linear finite depth theory. Each record was detrended to remove tidal effects, and ensemble averaging was used to form smoothed spectral estimates with 128 degrees of freedom and a frequency resolution of 0.0078 Hz. All time series considered (203 total) satisfy the condition that the linear energy flux (integrated over the frequency range 0.04–0.3 Hz) was within 15% of the flux concurrently measured in 8–9 m depth (i.e., breaking-induced dissipation was not significant). In the most shoreward records retained, waves were near breaking with steep forward faces and strong phase coupling between waves of different frequencies (Elgar and Guza 1985a,b; Elgar et al. 1997). Significant wave heights H_{sig} (four times the sea-surface elevation standard deviation) ranged from 20 to 180 cm, the frequency corresponding to the centroid of the power spectrum was between 0.071 and 0.185 Hz, and spectral widths [a nondimensional parameter related to the shape of the power spectrum (Longuet-Higgins 1975)] were between 0.037 and 0.264.

For each observed (target) power spectrum and bispectrum, 100 simulated time series were produced. The power spectra of the simulated time series are similar to the desired target (observed) values, with deviations mostly at high frequencies, as shown in Fig. 1(a) for a narrowband spectrum [H_{sig} = 1 m; h = 3.7 m; $b(0.07, 0.07)$ = 0.8; $b(0.07, 0.14)$ = 0.7; and NL = 0.70, where NL is defined in the following)]. Near the power-spectral primary peak frequency [f = 0.07 Hz, Fig. 1(a)] the simulated spectrum is nearly identical to the target spectrum. At frequencies corresponding to harmonics (f = 0.14 and f = 0.21 Hz) of the primary peak, the simulated spectral values are roughly 50% higher than observed, consistent with (10). As expected, the maximum differences between simulated and target power spectra are smaller for a broad-band wave field with smaller maximum bicoherence [H_{sig} = 0.6 m; h = 1.5 m; the maximum $b(f_l, f_m)$ = 0.4; and NL = 0.6] [Fig. 2(a)]. The bulk nonlinearity of the wave field is quantified here by $NL = \sqrt{S^2 + A^2}$, where S and A are sea-surface elevation skewness and asymmetry, third moments defined respectively as the mean cube of the time series and the mean cube of the Hilbert transform (a 90° phase shift) of the time series, each normalized by the 3/2-power of the variance (Elgar and Guza 1985b; Elgar 1987). The errors in total variance of the simulated time series (i.e., the integral of the power spectrum over frequency or, equivalently, the second moment) relative to observed values for all data sets are shown in Fig. 3. For small *NL*, simulated and observed total variance are nearly identical, and for the largest values of *NL* the difference is less than 20%.

Simulated [Figs. 1(d,e) and 2(d,e)] bispectra are similar to observed values (Figs. 1(b,c) and 2(b,c)]. Third moments (the real and imaginary parts of the bispectrum integrated over bi-

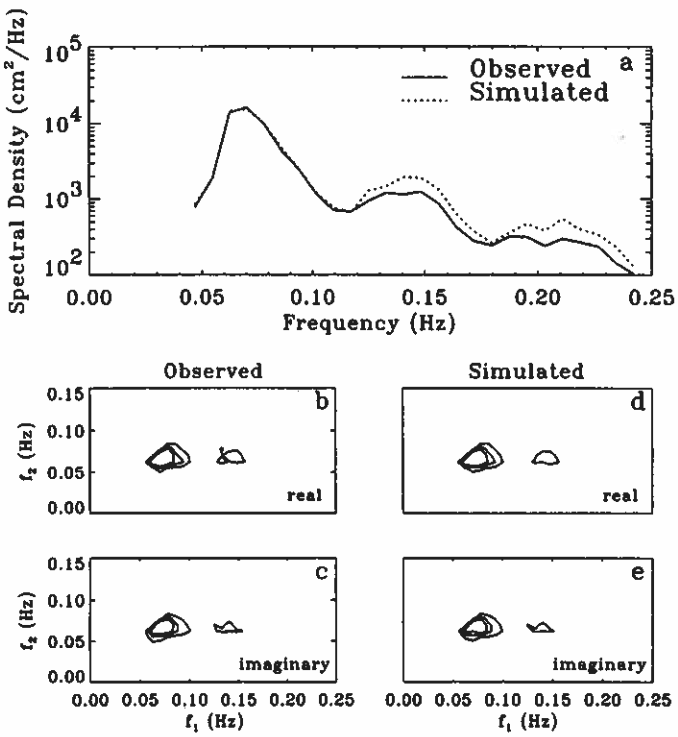

FIG. 1. Observed (Target) and Simulated (a) Power Spectral; and (b–e) Bispectral Density of Sea-Surface Elevation (Minimum Bispectral Contours Plotted Are $B = 10^5$ cm³/Hz², with Additional Contours Every 2×10^5 cm³/Hz²)

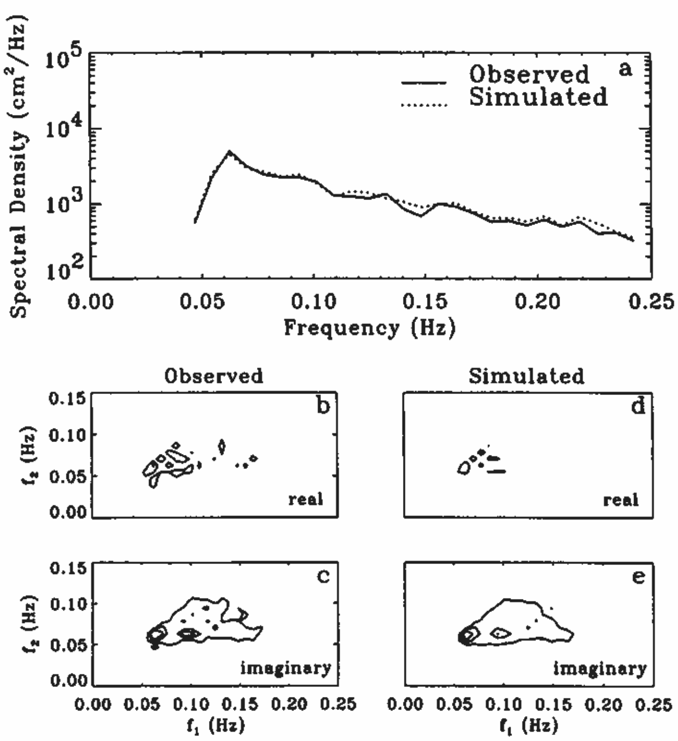

FIG. 2. Observed (Target) and Simulated (a) Power Spectral; and (b–e) Bispectral Density of Sea-Surface Elevation (Minimum Bispectral Contours Plotted Are $B = 0.25 \times 10^5$ cm³/Hz², with Additional Contours Every 0.5×10^5 cm³/Hz²)

frequency space) of the simulated wave fields are mostly within 20% of the target values (Fig. 4). For small values of *NL*, the error terms [(observed − simulated)/observed] can be large owing to a small denominator. Thus, data sets with approximately zero skewness and/or asymmetry ($|S|$, $|A| <$ 0.058, the 95% significance level estimated using random phase simulations of the 203 target power spectra) are not shown in Fig. 4. Overall, the simulated skewness and asymmetry are close to the observed values (Fig. 5, all data are shown). Gaussian simulations yield skewness and asymmetry values scattered around zero.

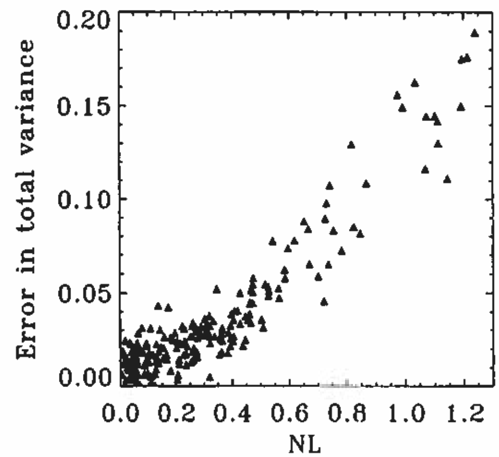

FIG. 3. Error [(Simulated − Observed)/Observed] in Total Variance (Second Moment) versus Observed *NL*

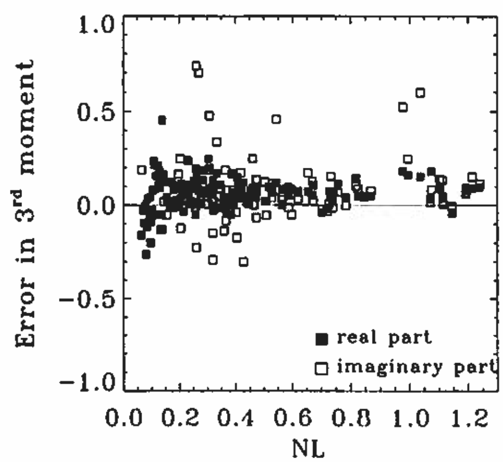

FIG. 4. Error [(Simulated − Observed)/Observed] in Real and Imaginary Third Moment versus Observed *NL*

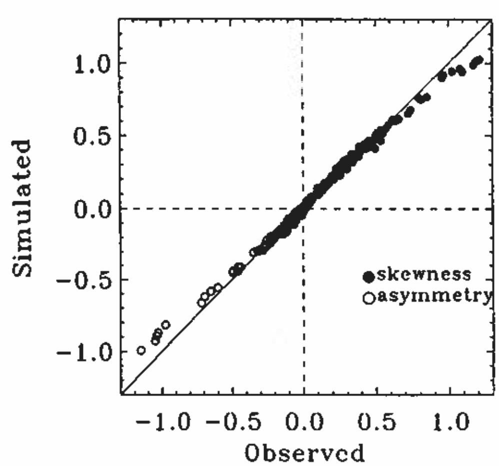

FIG. 5. Simulated versus Observed Skewness and Asymmetry

APPLICATION TO WAVE GROUPS

In deep and intermediate-depth water, the statistics of groups, or runs, of waves exceeding a particular height are usually consistent with a Gaussian sea surface and are simulated accurately with random phases [(1)] or random Fourier coefficients [(4)] (Andrew and Borgman 1981; Goda 1983; Elgar et al. 1984, 1985; Battjes and van Vledder 1984; Longuet-Higgins 1984; Thomas et al. 1986; Medina and Hudspeth 1990; Liu et al. 1993; and many others). However, in shallow water, deviations from a Gaussian sea surface are often significant and the mean length of groups (mean run length) of waves greater than the significant wave height increases, as shown in Fig. 6 (spectra and bispectra for this wave field in 3.7 m depth are shown in Fig. 1). The observed mean run lengths are larger than predicted by Gaussian simulations, and are more consistent with non-Gaussian simulations.

Mean run lengths from Gaussian and non-Gaussian simulations are compared to observed values for all data sets in Fig. 7. The scatter is large owing to the limited statistical stability of the individual observed run lengths (Elgar et al. 1984). For small nonlinearity *NL* both simulation methods predict accurately the observed mean run lengths (Fig. 8, where individual data points are accumulated into *NL* bins 0.2 wide and are plotted at the bin midpoint). As *NL* increases, errors in both simulations increase, but errors in the Gaussian simulated run lengths are twice as large as errors in the non-Gaussian simulations.

Mean run lengths are well known to increase with increasing spectral width (Goda 1983; and many others), but mean run lengths also increase with increasing nonlinearity, as shown in Fig. 9 (where individual data points are accumulated into *NL* bins 0.2 wide). After removing the effect of spectral width, the partial correlation coefficient (0.56) between the 203 observed mean run lengths and *NL* is significant at the 99% level (Jenkins and Watts 1968).

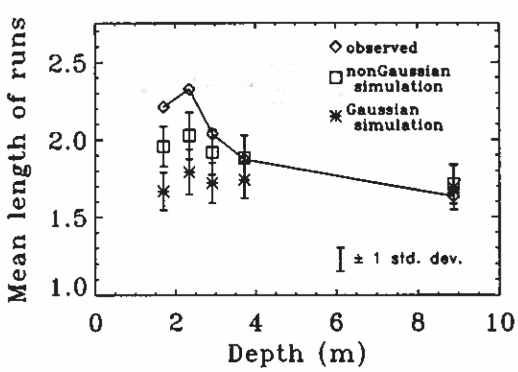

FIG. 6. Mean Length of Runs of Consecutive Waves Greater than Significant Wave Height versus Depth

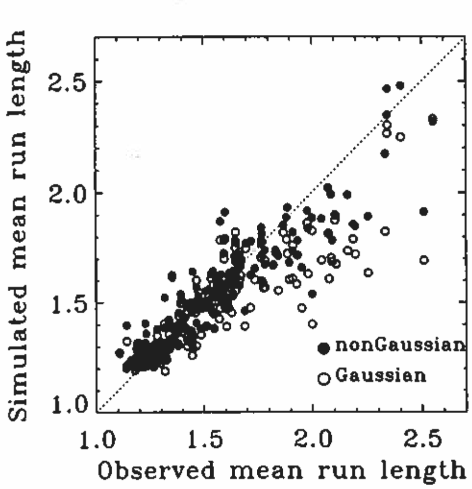

FIG. 7. Simulated versus Observed Mean Run Lengths

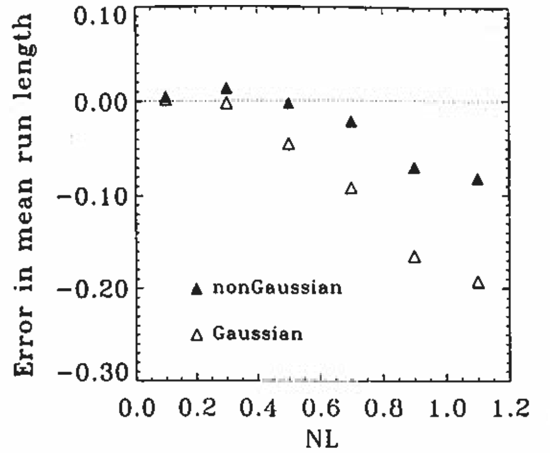

FIG. 8. Error [(Simulated – Observed)/Observed] in Mean Run Length versus Observed *NL*

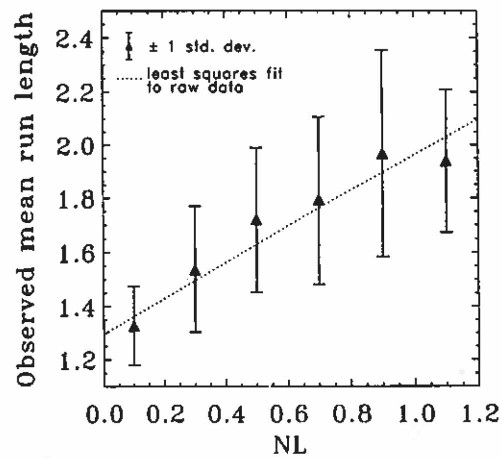

FIG. 9. Observed Mean Run Length versus Observed *NL*

To examine further the effect of nonlinearity on mean run length, non-Gaussian sea surfaces with identical spectral widths, but with different *NL*, were simulated. For a particular observed spectra and bispectra, the range of *NL* was obtained by scaling the target bispectrum by a factor $0 \le \alpha \le 1.5$. The simulation methodology was altered slightly to eliminate errors in the power spectrum owing to the second term on the right-hand side of (7), thus producing simulated time series with constant spectral width and variable *NL*. The Fourier coefficients of the simulated time series are given by

$$\hat{X}(f_k) = \hat{G}(f_k) + \sum_{f_l=-f_N}^{f_N} \alpha Q(f_l, f_k - f_l)\hat{G}(f_l)\hat{G}(f_k - f_l); \quad -f_N \le f_k \le f_N \tag{12}$$

which yields power spectra

$$\hat{P}(f_k) = \hat{P}_G(f_k) + \sum_{f_l=-f_N}^{f_N} \alpha^2 |Q(f_l, f_k - f_l)|^2 \hat{P}_G(f_l)\hat{P}_G(f_k - f_l);$$

$$-f_N \le f_k \le f_N \tag{13}$$

where $\hat{G}(f_k)$ = Fourier coefficients of the Gaussian simulation with power spectrum $\hat{P}_G(f_k)$ chosen using nonlinear minimization (Gill and Murray 1978) such that the simulated power spectrum $\hat{P}(f_k)$ [i.e., (13)] is identically equal to the target power spectrum $P(f_k)$. Although errors in the simulated power spectrum (and in the total variance, Fig. 3) are eliminated, additional errors are introduced into the simulated bispectrum.

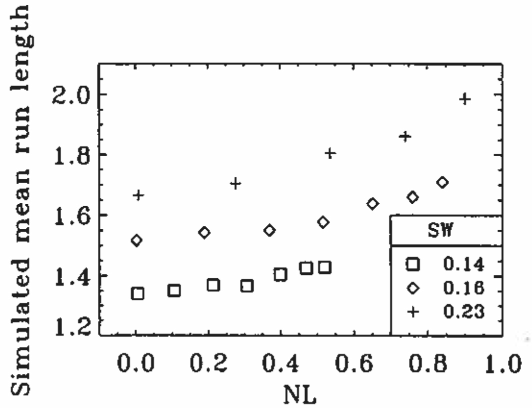

FIG. 10. Mean Run Length in Simulated Non-Gaussian Time Series versus *NL*

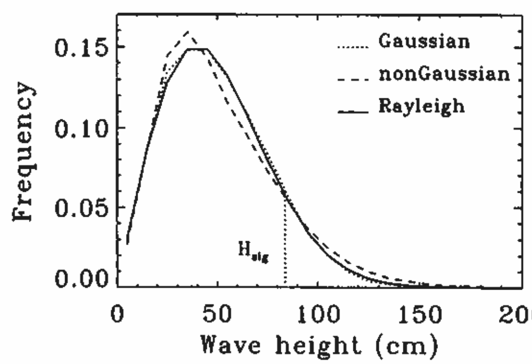

FIG. 11. Frequency of Occurrence of Wave Height versus Wave Height

Results of simulations for three spectral widths (SW) were similar. As α ranged from 0 to 1.5, *NL* ranged from 0 to 0.9, and the mean run length increased (Fig. 10). The distribution of wave heights (Fig. 11 for the SW = 0.23 case in Fig. 10), as well as mean run length, changes with increasing *NL*. The simulated Gaussian (*NL* = 0) wave heights are close to Rayleigh distributed [the theoretical distribution for a linear, narrowband process (Longuet-Higgins 1952)], but when *NL* = 0.9 the simulations differ significantly (99% level) from Rayleigh (Fig. 11). The percentage of wave heights greater than the significant wave height is smaller for the Gaussian (11%) than for the non-Gaussian (14%) simulations, consistent with the relatively shorter runs of large waves in the Gaussian simulations.

CONCLUSIONS

A method to simulate non-Gaussian time series with a specified (target) power spectrum and bispectrum reproduces accurately the observed second- and third-order statistics of nonbreaking, shoaling waves. Although the deviations between simulated and target power spectra and bispectra increase as the nonlinearity of the wave field increases, the total variance and normalized third moments (skewness and asymmetry) of the simulated non-Gaussian sea surfaces were in all cases within about 20% of their targets. Gaussian simulations have vanishing third moments. As the nonlinearity increases, the mean lengths of groups (runs) of high waves observed in shallow water (less than 9 m depth) diverge from the predictions of both Gaussian and non-Gaussian simulations, but are predicted more accurately by non-Gaussian simulations. The simulations suggest that quadratic nonlinearity causes an observed shoreward increase in the mean run lengths of shoaling waves.

ACKNOWLEDGMENTS

This research was supported by the Office of Naval Research (Coastal Dynamics and AASERT graduate student support), the Naval Research Laboratory, and the National Science Foundation (CoOP program). The field data were obtained in collaboration with E. B. Thornton (Santa Barbara) and E. Gallagher, T. H. C. Herbers, and B. Raubenheimer (Duck).

APPENDIX. REFERENCES

Andrew, M. E., and Borgman, L. E. (1981). "Procedures for studying wave grouping in wave records from California Coastal Data Collection Program." *Rep.*, U.S. Army Corps of Engrs., San Francisco, Calif., Nov.

Battjes, J. A., and van Vledder, G. P. (1994). "Verification of Kimura's theory for wave group statistics." *Proc., 19th Int. Coast. Engrg. Conf.*, ASCE, New York, N.Y., 642–648.

Elgar, S., and Chandran, V. (1993). "Higher-order spectral analysis to detect nonlinear interactions in measured time series and an application to Chua's circuit." *Int. J. Bifurcation and Chaos*, 3, 19–34.

Elgar, S., and Guza, R. T. (1985a). "Shoaling gravity waves: comparisons between field observations, linear theory, and a nonlinear model." *J. Fluid Mech.*, 158, 47–70.

Elgar, S., and Guza, R. T. (1985b). "Observations of bispectra of shoaling surface gravity waves." *J. Fluid Mech.*, 161, 425–448.

Elgar, S., Guza, R. T., Raubenheimer, B., Herbers, T. H. C., and Gallagher, E. (1997). "Spectral evolution of shoaling and breaking waves on a barred beach." submitted to *J. Geophys. Res.*

Elgar, S., Guza, R. T., and Seymour, R. (1984). "Groups of waves in shallow water." *J. Geophys. Res.*, 89, 3623–3634.

Elgar, S., Guza, R. T., and Seymour, R. (1985). "Wave group statistics from numerical simulations of a random sea." *Appl. Oc. Res.*, 7, 212–237.

Gill, P. E., and Murray, W. (1978). "Algorithms for the solution of the nonlinear least-squares problem." *SIAM J. Numer. Anal.*, 15, 977–992.

Goda, Y. (1983). "Analysis of wave grouping and spectra of long-traveled swell." *Rep. 22*, Port and Harb. Res. Inst., Nagase, Yokosuka, Japan, 3–41.

Haubrich, R. A. (1984). "Earth noise, 5 to 500 millicycles per second." *J. Geophys. Res.*, 70, 1415–1427.

Hasselmann, K., Munk, W., and MacDonald, G. (1963). "Bispectra of ocean waves." *Time Series Analysis*, M. Rosenblatt, ed., Wiley, New York, N.Y., 125–139.

Jenkins, G., and Watts, D. (1968). *Spectral analysis and its applications.* Holden-Day, San Francisco, Calif.

Kim, Y. C., and Powers, E. J. (1979). "Digital bispectral analysis and its applications to nonlinear wave interactions." *IEEE Trans. on Plasma Sci.*, 7, 120–131.

Liu, Z., Elgar, S., and Guza, R. T. (1993). "Groups of ocean waves: Comparisons between linear theory, approximations to linear theory, and observations." *J. Wtrwy., Port, Coast., and Oc. Engrg.*, ASCE, 119(2), 144–159.

Longuet-Higgins, M. S. (1952). "On the statistical distribution of the heights of sea waves." *J. Marine Res.*, 9, 245–266.

Longuet-Higgins, M. S. (1975). "On the joint distribution of the periods and amplitudes of sea waves." *J. Geophys. Res.*, 80, 2688–2694.

Longuet-Higgins, M. S. (1984). "Statistical properties of wave groups in a random sea state." *Philosophical Trans. Royal Soc.*, London, U.K., Ser. A, 312, 219–250.

Medina, J. R., and Hudspeth, R. T. (1990). "A review of the analysis of ocean wave groups." *Coast. Engrg.*, 14, 515–542.

Nikias, C. L., and Raghuveer, M. R. (1987). "Bispectral estimation: A digital signal processing approach." *Proc., IEEE*, 75, 869–891.

Rice, S. O. (1954). "Mathematical analysis of random noise." *Selected papers on noise and stochastic processes*, N. Wax, ed., Dover Publications, Inc., New York, N.Y.

Schetzen, M. (1980). *The Volterra and Wiener theories of nonlinear systems*. Wiley, New York, N.Y.

Thomas, K., Baba, M., and Harish, C. (1986). "Wave groupiness in long-traveled swell." *J. Wtrwy., Port, Coast., and Oc. Engrg.*, ASCE, 112(4), 498–511.

Vanhoff, B., and Elgar, S. (1997). "Simulating quadratically nonlinear random processes." *Int. J. Bifurcation and Chaos*, in press.